Optimal Design of Hybrid Battery Energy Storage System for Minimizing the Number of Batteries with High Efficiency Control Algorithm based on Fuzzy Logic

Tae-Won Noh, Jung-Hoon Ahn, Hyo Min Ahn, and Byoung Kuk Lee
Department of Electrical and Computer Engineering
Sungkyunkwan University
Suwon, Republic of Korea
bkleeskku@skku.edu

***Abstract*—This paper proposes the optimization method and the control algorithm for hybrid battery energy storage system (HBESS) by combination of the high energy battery and high power battery. The proposed design method minimizes the total number of the batteries through the cost function. The control algorithm for high efficiency is composed of fuzzy logic controller (FLC) so as to reflect the various control conditions and the dynamic characteristics of battery. Finally, the proposed design method and algorithm are validated through informative simulation based on experimental results.**

Keywords—hybrid battery energy storage system (HEBSS); fuzzy; battery management; optimal design

I. INTRODUCTION

The increasing needs for the reduction of energy costs and the improvement of power quality have accelerated the development of battery energy storage systems (BESS)[1-3]. The battery capacity should be minimized for the economical and compact design of BESS while also satisfying the demand of BESS (D_{BESS}) which consists of maximum power and maximum energy of the power demand profile. The performances of the battery module in BESS can be represented in the energy-power plane by a unit vector which indicates the guaranteed power ability and the energy storage capacity like in Fig. 1. The number of battery modules is directly proportional to the length of design vector (v_d) determined by accumulating the unit vector until D_{BESS} is satisfied as shown in Fig. 1. Thus, the length of v_d should be reduced in order to minimize the number of batteries.

Fig. 2 is a Ragone plot which represents the performance of the batteries used for BESS by plotting the energy and power characteristics at the coordinate plane. The x-axis of the Ragone plot means the energy storage ability and y-axis indicates the power performance which is calculated by multiplication of continuous current and minimum voltage of each battery. As shown in Fig. 2, the types of battery can be categorized into two groups: the high energy battery (B_e) and the high power battery (B_p). The battery types which are distributed near the x-axis belong to B_e and the types of B_p are around the y-axis. The

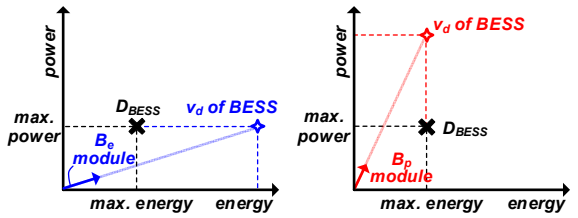

(a) General BESS using B_e (b) General BESS using B_p

Fig. 1. Example of design for BESS using single type of battery.

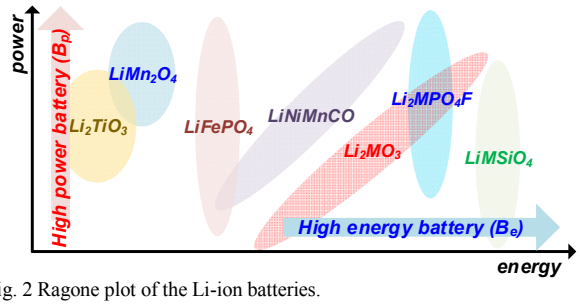

Fig. 2 Ragone plot of the Li-ion batteries.

general BESS using a single type of battery needs large amounts of batteries to meet D_{BESS} because of the performance deviation between the power and energy ability as shown in Fig. 1. In order to solve this problem, the hybrid battery energy storage system (HBESS) which performs the BESS function by using B_e and B_p together is necessary. In HBESS, B_e is responsible for the continuous base load and B_p satisfies the instantaneous peak load. Fig. 3 shows that HBESS can meet the D_{BESS} with a smaller amounts of battery than general BESS using just a single type of battery.

In literature, the design and control algorithm for BESS using ultra-capacitor (UC) with the battery have been researched[4-6]. However, UC can be inappropriate to various applications because it has a small energy storage capacity in contrast to power performance. And the conventional researches for HBESS propose the concepts for just combining the lead

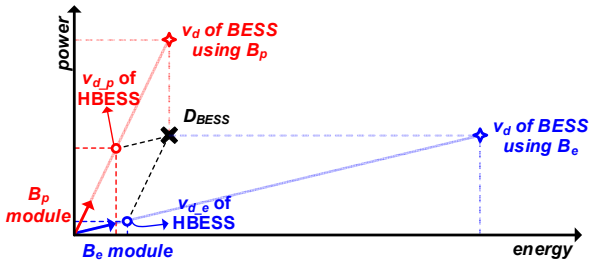

Fig. 3. Design of HBESS using two types batteries (B_e, B_p).

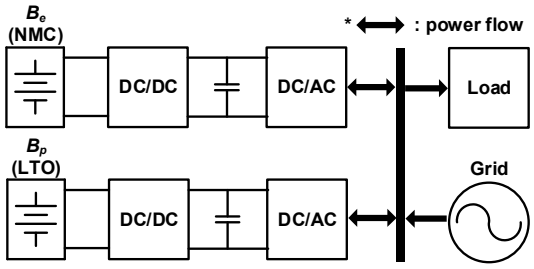

Fig. 4. HBESS configuration and power flow.

TABLE I. SPECIFICATIONS OF BATTERIES USED IN HBESS

Contents	Batteries used in HBESS	
	Energy Battery (B_e)	Power Battery (B_p)
Model (Type)	SLPB776495 (NMC)	SLPB1330255255N (LTO)
Manufacturer	Kokam	Kokam
Capacity	5.3 Ah	60 Ah
Discharge rate	2 C	6 C
Energy density	192 Wh/kg	76 Wh/kg
Volume	48,046 mm^3	895,462 mm^3

acid battery with Li-ion battery and these researches are limited in the optimization because the changes of characteristics of the battery according to the operation conditions like voltage range, allowable current and state of charge (*SOC*) are not considered [7]. Moreover, because HBESS uses the dual batteries unlike general BESS, the control algorithm for HBESS should consider both SOCs of B_e and B_p to prevent the over-charge and over-discharge. At the same time, this algorithm has to take into account the charging and discharging loss caused by the internal resistance varied with *SOC* for the high efficiency[8-9].

This paper proposes a comprehensive solution for HBESS by the optimized design method to determine the number of batteries and the control algorithm for the efficient and stable operation of HBESS. The proposed design method uses a cost function considered the volume, cost and utilization of HBESS. Moreover, the changes of the battery characteristics by the operating conditions are considered to improve the optimization of the number of batteries. The control algorithm is made up of the fuzzy logic so as to reflect the various control factors simultaneously: the power demand, SOC of each battery and the efficiency of HBESS. The feasibilities of the proposed design method and control algorithm are verified by the simulation results based on the specifications of the batteries and experimental results.

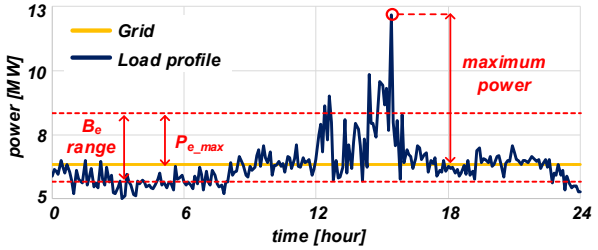

(a) Power demand profile.

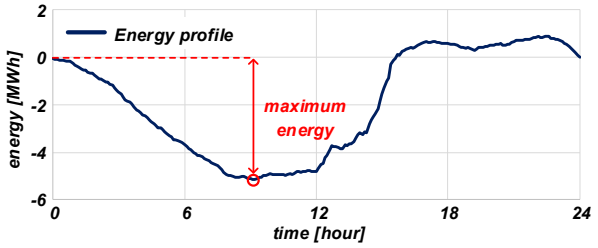

(b) Energy profile calculated by integration of power load in (a)

Fig. 5. Load profiles used to design HBESS.

II. OPTIMIZED DESIGHN METHOD TO DETERMINE NUMBER OF BATTERIES FOR HBESS

A. Optimization method using cost function

Fig. 4 is the configuration of the HBESS and represents the power flow between the batteries (B_e and B_p), load and grid. The voltages and currents of B_e and B_p are controlled by power conversion systems in order to satisfy the power demand of HBESS. NMC (Lithium Nickel Manganese Cobalt Oxide)-type battery is used for B_e (SLPB776495) and B_p consists of LTO (Lithium Titanate Oxide)-type battery (SLPB1330255255N) manufactured by Kokam. The specifications are described in Table I[10-11].

Fig. 5(a) is the power demand profile used in this paper[12]. It is assumed that grid supplies the average value of the power demand for load leveling and HBESS provides the remainder of the power demand except of the grid. D_{BESS} of HBESS is determined by maximum power and energy of the demand profile shown in Figs. 5(a) and (b). B_e of HBESS covers the base load which is belong to the specific power range and the instantaneous peak power demands beyond this power range are satisfied by B_p.

The design points of each battery (D_e, D_p) and the number of the batteries are dependent on the supplying power range of B_e. Therefore, the power range of B_e should be considered in order to optimize the number of the batteries. In this paper, the minimum supplying power of B_e is fixed at 5.66MW and the optimal value of the maximum supplying power (P_{e_max}) is deduced by the proposed optimization method. The considered conditions for design of HBESS are volume (v), cost (c) and utilization of each battery (u). The utilization means the ratio of power (or energy) demand to the designed capacity of power (or energy). In order to induce the optimal point of P_{e_max}, the cost function (f_c) is defined as the sum of ratio of v, c and u like (1). The high value of f_c means that HBESS is optimized and f_c can

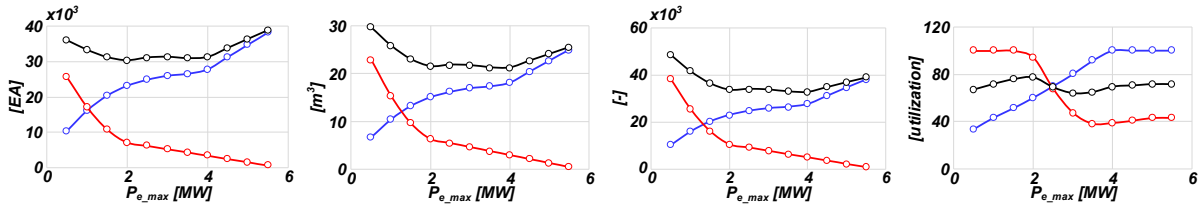

(a) number (b) volume (c) cost (normalized by 1 cell of B_e) (d) utilization

Fig. 6. HBESS characteristics following P_{e_max}.

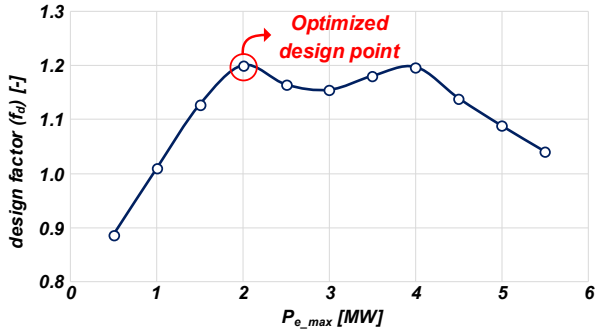

Fig. 7. f_c for HBESS optimization and optimized value of P_{e_max}.

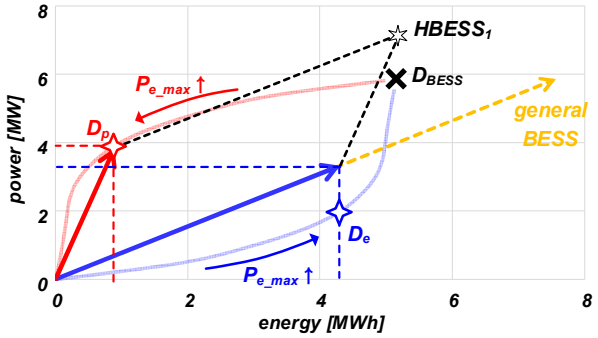

Fig. 8. Comparison of design points of $HBESS_1$ to general BESS.

reflects the characteristic of application by manipulating the influence rates of each component (α_x).

$$f_c = \alpha_v \frac{v_{BESS}}{v_{HBESS}} + \alpha_c \frac{c_{BESS}}{c_{HBESS}} + \alpha_u \frac{u_{BESS}}{u_{HBESS}} \quad (1)$$

Fig. 6 shows the analysis results of the components influencing on f_c according to P_{e_max}. The number of the batteries has the minimum value when P_{e_max} is 2 MW and the volume and cost of HBESS have a similar tendency to the number of batteries. The cost factor is calculated with the assumption that B_p is one and half times higher than B_e because LTO is developed recently against the NMC. The costs of each battery and total cost are represented in Fig. 6(c) in being normalized by the cost of B_e. The utilization of the battery has the highest value when P_{e_max} is 2 MW. Through these analysis results, the optimization point of P_{e_max} is induced to 2 MW like in Fig. 7 and the design result of HBESS is shown in Fig. 8 as $HBESS_1$.

B. *Optimization for Slope of v_d by Using Dynamic Characteristics of Battery*

As shown in Fig. 8, though $HBESS_1$ is optimized by f_c, $HBESS_1$ does not satisfy the power and energy demand correctly because the inherent slope of v_d cannot be changed. Thus, the additional optimization process limits the operating voltage and current of the battery in order to meet the D_{BESS} more correctly through an adjustment of the slope of v_d.

Generally, the current capacity of the battery is defined as the amount of total charges flowed out from the battery when the battery is discharged from *SOC* 100% to when the terminal voltage reaches to the lower limitation value. The terminal voltage of the battery on discharge is described by the subtraction of voltage drops, V_{ohm} and V_{diff}, generated by the internal impedances from open circuit voltage (*OCV*) as shown in Fig. 9 and (2). Thus, the terminal voltage would reach to the lower limitation value before fully discharged because of these additional voltage drops. Given that these voltage drops are proportional to the terminal current like in (2), the current capacity can be improved by reducing the maximum operating current of the battery as shown in Fig. 10(a) but the power ability is degraded. This method makes the slope of v_d become a little steep.

$$\begin{aligned} v_{terminal} &= OCV - V_{ohm} - V_{diff} \\ &= OCV - i_{terminal} \cdot R_{ohm} - V_{diff} \end{aligned} \quad (2)$$

And another way to change the slope of v_d is increasing the minimum voltage of the battery to make the power ability higher as shown in Fig. 10 (b) while the energy ability is decreased. The guaranteed power of the battery is determined by the multiplication of the maximum continuous current and lower limit voltage. Thus, increasing the lower limit value of terminal voltage raises the guaranteed power more higher than general one while available energy density is decreased, which means that the slope of v_d increases.

As shown in Fig. 11, the slope of B_e is declined by limiting

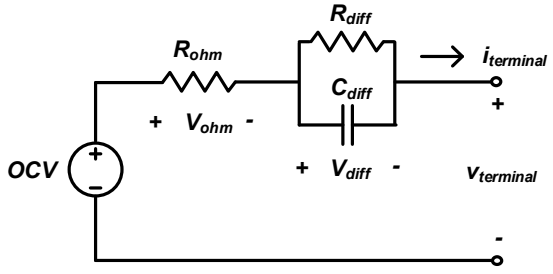

Fig. 9. Equivalent circuit model of battery: 1st RC-ladder model.

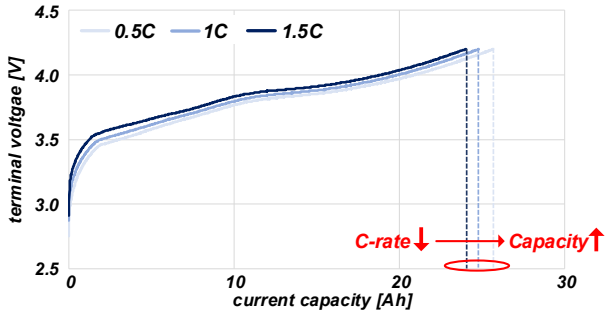

(a) Enhancement of current capacity by limitation of current

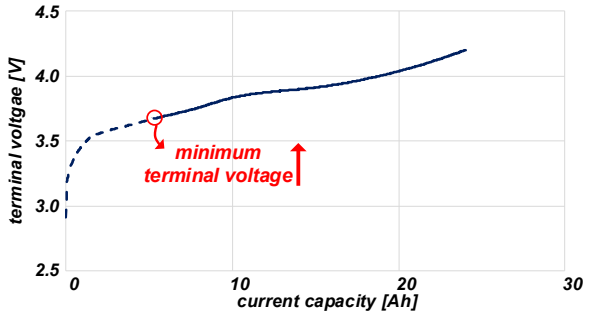

(b) Improvement of minimum power through limitation of voltage

Fig. 10. Additional optimization by control of battery operating condition.

the allowable current and the slope of B_p becomes a little steep through adjusting the minimum voltage. In Fig. 12, the number of batteries of HBESS which is optimized by the proposed methods ($HBESS_{opt.}$) are compared with general BESS using a single type of battery and $HBESS_1$ ignoring the battery characteristics. $HBESS_{opt.}$ needs just 61.05% of the number of batteries compared to the general BESS and the volume, cost and utilization of the HBESS are enhanced better than general BESS as shown in Table II.

III. Control Algorithm for High Efficient Operation of HBESS

The control algorithm for HBESS should determine the amounts of charging and discharging power of each battery in consideration of lots of conditions like power demand, *SOC* of each battery and charging and discharging efficiency of battery for stable and efficient operation. The proposed algorithm uses the fuzzy logic controller (FLC) suitable to solve the uncertainty of the relation between lots of consideration.

Basically, the algorithm distributes the power demands to each battery according to the supplying power range which is determined by the optimization design method. In order to enhance the charging and discharging efficiency of the battery, the internal resistance which is varied with *SOC* like in Fig. 13 should be considered because the efficiency is inversely proportional to the internal resistance. Thus, the proposed control algorithm makes B_p supply some power though the magnitude of the power demands are in the range of B_e so as to make the *SOC* of each battery the maximum efficiency point (SOC_{η_max}).

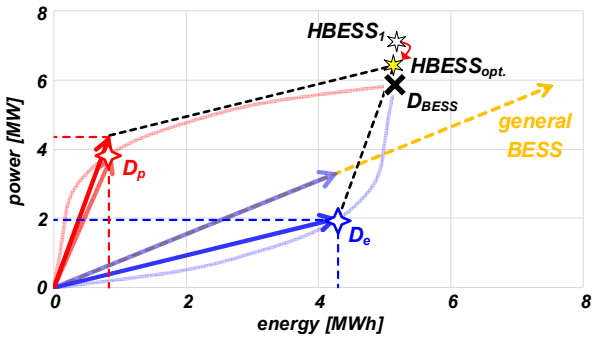

Fig. 11. Additional optimization and design point of $HBESS_{opt.}$.

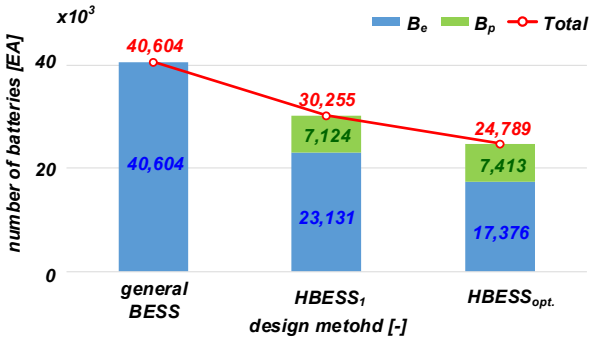

Fig. 12. Comparison of the number of batteries following design method.

TABLE II. Comparison of Characteristics of HBESS

HBESS type	Number of batteries [EA]	Volume [m^3]	Cost [-]	Utilization [%]
General BESS	40,604	26.51	40,604	68.14
$HBESS_1$	30,255	21.48	33,817	77.10
$HBESS_{opt.}$	24,789	17.98	28,496	99.61

As shown in Fig. 13, if *SOC* is lower than SOC_{η_max} (SOC_{case1}), FLC increases the amount of charging power and decreases the discharging power. In reverse case (SOC_{case2}), FLC makes the battery discharged more by increasing the supplying power and decreasing the discharging power. Figs. 14(a) and (b) show a flow chart of the control algorithm, membership functions and rule bases of the FLC. In order to verify the proposed algorithm, the simulation is carried out by using the charging efficiency data extracted by using the charger

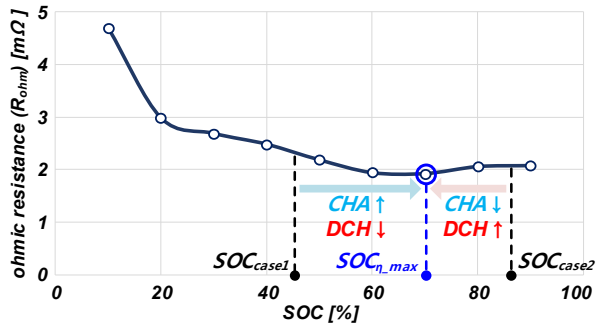

Fig. 13. Internal resistance of NMC battery and main principle of FLC.

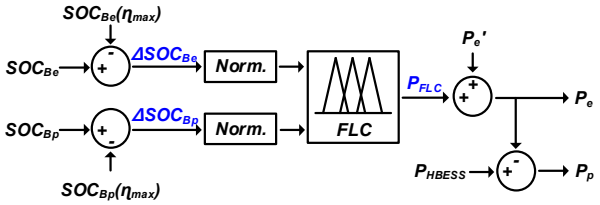

(a) Flow chart of proposed control algorithm

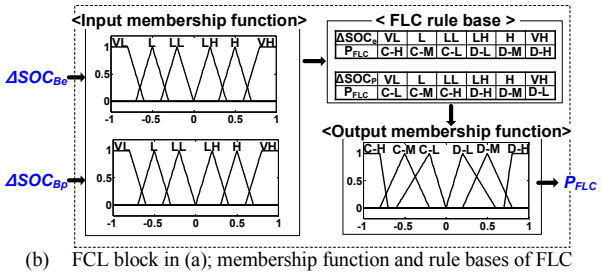

(b) FCL block in (a); membership function and rule bases of FLC

Fig. 14. Proposed control algorithm using FLC.

and discharger in Fig. 15. Fig. 16 is the simulation results of the proposed control algorithm. The distribution of the power demand is determined by maximizing the charging and discharging efficiency of the batteries. The efficiency is calculated by using the internal resistances and terminal current of the batteries and the average value of efficiency between B_e and B_p is used for verification. The average efficiency for 1 cycle of power demand profile is 92.71% when the proposed algorithm is used. This efficiency is 2.54% higher than the general power distribution which considers just power range of each battery.

IV. Conclusions

In this paper, the optimized design method and the control algorithm of HBESS are proposed for the comprehensive solution for HBESS. The proposed design method optimizes the number of the batteries by defining the cost function for system features and considering the dynamic characteristic of both batteries. The control algorithm using the fuzzy logic enhances the charging and discharging efficiency of both batteries through control of power distribution to both batteries. The feasibilities of the proposed method and algorithm are verified with the simulations based on the specifications of the real batteries and the efficiency data extracted by experiments.

Acknowledgment

This work was supported by the Industrial Strategic Technology Development Program (No.10053710) funded by the Ministry of Trade, Industry & Energy(MI, Korea).

References

[1] Y. Zheng, Z. Y. Dong, F. J. Luo, K. Meng, J. Qiu, and K. P. Wong. "Optimal allocation of energy storage system for risk mitigation of DISCOs with high renewable penetrations," *IEEE Trans. Power Syst.*, vol. 29, no. 1, pp. 212-220, Jan. 2014.

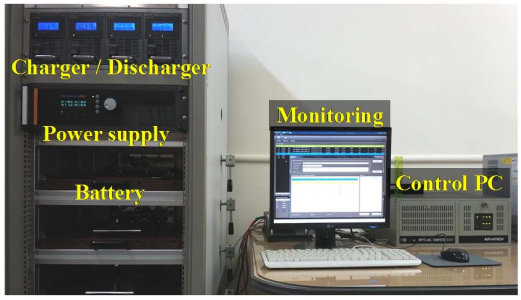

Fig. 15. Experiment set-up for identification of batteries cell.

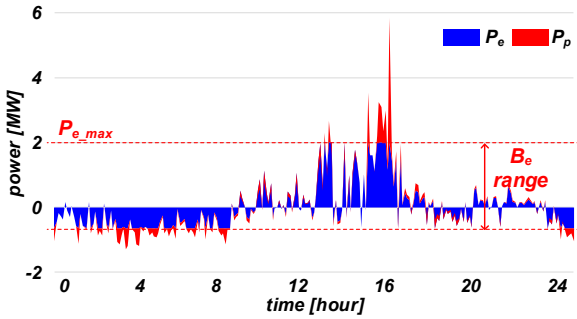

Fig. 16. Simulation results of proposed control algorithm.

[2] R. Bass, J. Carr, J. Aguilar and K. Whitener, "Determining the power and energy capacities of a battery energy storage system to accommodate high photovoltaic penetration on a distribution feeder," *IEEE J. Power and Energy Technology Syst.*, vol. 3, pp. 119-127, Sep. 2016.

[3] Y. Guan; J. Vasquez; J. Guerrero, "Coordinated Secondary Control for Balanced Discharge Rate of Energy Storage System in Islanded AC Microgrids," *IEEE Trans. Ind. Appl.*, vol. 52, no. 6, pp. 5019-5028, Aug. 2016.

[4] J. Shen and A. Khaligh, "Design and real-time controller implementation for a battery-ultracapacitor hybrid energy storage system," *IEEE Trans. Ind. Informat.*, vol. 12, no. 5, pp. 1910–1918, Oct. 2016.

[5] A. Ostadi and M. Kazerani, "A comparative analysis of optimal sizing of battery-only, ultracapacitor-only, and battery–ultracapacitor hybrid energy storage systems for a city bus. vehicular technology," *IEEE Trans. Veh. Technol.*, vol. 64, no. 10, pp. 4449–4460, Oct. 2015.

[6] D. B. W. Abeywardana, B. Hredzak, and V. G. Agelidis, "Single-phase grid-connected LiFePO4 battery–supercapacitor hybrid energy storage system with interleaved boost inverter," *IEEE Trans. Power Electron.*, vol. 30, no. 10, pp. 5591–5604, Oct. 2015.

[7] K. Takeda, C. Takahashi, H. Arita, N. Kusumi, M. Amano, and A. Emori, "Design of hybrid energy storage system using dual batteries for renewable applications," *in Proc. IEEE Power Energy Soc. (PES) General Meeting Conf. Expo.*, Jul. 2014, pp. 1–5.

[8] Z. Chen, B. Xia, C. C. Mi, and R. Xiong, "Loss-minimization-based charging strategy for lithium-ion battery," *IEEE Trans. Ind. Appl.*, vol. 51, no. 5, pp. 4121–4129, Mar. 2015.

[9] H. Qian, J.H. Zhang, J.-S. Lai, and W.S. Yu, "A High-Efficiency Grid-Tie Battery Energy Storage System", *IEEE Trans. Power Electron.*, vol. 26, no.3, pp. 886–896, May. 2011.

[10] A. I. Stan, M. Swierczynski, D. I. Stroe, R. Teodorescu, S. J. Andreasen, and K.Moth, "Acomparative study of lithium ion to lead acid batteries for use in UPS applications," *in Proc. 2014 IEEE Int. Telecommun. Energy Conf.*, pp. 1–8.

[11] N. Omar et al., "Assessment of performance of lithium iron phosphate oxide, nickel manganese cobalt oxide and nickel cobalt aluminum oxide based cells for using in plug-in battery electric vehicle applications," *in Proc. IEEE Veh. Power Prop. Conf.*, Sep. 2011, pp. 1–7.

[12] W. J. Kim (2017, Mar 08). [Online]. Available: http://www.kpx.or.kr/www/contents.do?key=83